

agonal phase with a c/a ratio of 1.009, which are almost agree with the results reported by King and Goo.¹⁴ They reported that c/a ratio was 1.01 for BaTiO_3 and was decreased with increasing calcium content in $\text{Pb}_{1-x}\text{Ca}_x\text{TiO}_3$. As greater amount of strontium added, the phase moves from the tetragonal phase to the cubic. For $x=0.3$, the crystal structure of $\text{Ba}_{0.7}\text{Sr}_{0.3}\text{TiO}_3$ clearly shows the cubic (or pseudocubic) phase. The unit cell volume was decreased with increasing amount of strontium substitution to barium sites. As reported by Park *et al.*,¹⁵ the unit cell volume was also linearly decreased by increasing the amounts of strontium addition to barium sites in $\text{Ba}_{1-x}\text{Sr}_x\text{Ti}_{0.995}\text{Ca}_{0.005}\text{O}_{2.995}$. The radius of strontium ion is smaller than that of the barium ion. The change of the unit cell volume shown in Figure 6 was due to the substitution of strontium to the barium sites. The decrease of c/a ratio and unit cell volume along with the amount of strontium substitution to the barium sites shows that the strontium ion was completely substituted to the barium sites up to 30 mol% by the revised oxalate coprecipitation method at room temperature.

Acknowledgment. The present studies were supported by of Basic Science Research Institute Program, Ministry of Education, 1995. Project No. BSRI-95-3439.

References

1. Clabaugh, W. S.; Swiggard, E. M.; Gilchrist, R. J. *Res.*

- Natl. Bur. Stand.(U.S.)* 1956, 56, 289.
2. Gallagher, P. R.; Schrey, F.; Dimarcello, F. V. *J. Am. Ceram. Soc.* 1963, 46, 359.
3. Schrey, F. *J. Am. Ceram. Soc.* 1965, 48, 401.
4. Fang, T. T.; Lin, H. B. *J. Am. Ceram. Soc.* 1989, 72, 1899.
5. Furman, N. H. *Standard Methods of Chemical Analysis*; van Nostrand Comp.: Princeton, U.S.A., 1962.
6. Yamamura, H.; Watanabe, A.; Shirasaki, S.; Moriyoshi, Y.; Tanada, M. *Ceram. Int.* 1985, 11, 17.
7. Kim, S.; Choi, S. W.; Huh, W. Y.; Czae, M. Z.; Lee, C. *Bull. Kor. Chem. Soc.* 1993, 14, 38.
8. Cullity, B. D. *Elements of X-ray Diffraction*; Addison-Wesley Pub. Comp.: Massachusetts, 1978.
9. Smith, R. M.; Martel, A. E. *Critical Stability Constants*; Plenum Press: New York, 1977.
10. *CRC Handbook of Chemistry and Physics*; 60th ed., CRC Press: 1979, pB-220.
11. Vasil'ev, V. P.; Vorob'ev, P. N.; Khodakovskii, I. L. *Russ. J. Inorg. Chem.* 1974, 19, 1481.
12. Turner, D. G.; Whitfield, M.; Dickson, A. G. *Geochim. Cosmochim. Acta* 1981, 45, 855.
13. Babko, A. K.; Dubovenko, L. I. *Chemical Abstract* 1959, 53, 17745e.
14. King, G.; Goo, E. K. *J. Am. Ceram. Soc.* 1990, 73, 1534.
15. Park, J. G.; Oh, T. S.; Kim, Y. H. *J. Mater. Sci.* 1992, 27, 5713.

Rapid Quenching Dynamics of F Center Excitation by OH^- Defects in KCl

Du-Jeon Jang*[†] and Pilseok Kim

Department of Chemistry, Seoul National University, Seoul 151-742, Korea

[†]*Also a member of the Center for Molecular Science, Taejon 305-701, Korea*

Received August 16, 1995

The rapid quenching dynamics of F center excitation by OH^- defects in KCl crystals are investigated by monitoring ground state absorption bleach recovery, using a picosecond streak camera absorption spectrometer. F center absorption bleach in OH^- -doped crystals shows three distinguishable recovery components with the current temporal resolution, designated as slow, medium and fast components. The slow one is due to the normal relaxation process of F^* centers as found in OH^- -free crystals. The others are consequent on energy transfer from electronically excited F centers to OH^- -vibrational levels. The fast component is a minor energy transfer process and resulting from the relaxation of somewhat distant, not the closest, associated pairs of F^* and OH^- defects. The energy transfer between widely separated F^* and OH^- defects opens up a recovery process *via* the medium component which is assisted by OH^- librations, lattice vibrations and OH^- dipole reorientations. The quenching behaviors of F^* luminescence and photoionization by OH^- are explained well by the relaxation process of the medium component.

Introduction

Electronically excited F centers in alkali halides relax lattice-vibrationally within a few picoseconds at cryogenic temperature into the relaxed excited state.¹ The relaxed excited F centers (F^* centers) decay *via* radiative and nonradiative

transitions to the ground state and through ionization to the conduction band.² F^* centers usually emit a highly efficient, spectrally broad, long-lived and largely Stokes-shifted luminescence at cryogenic temperature,³ although the radiative quantum efficiency depends on host.⁴ F^* centers in potassium and rubidium halides have good radiation efficiencies close

to one and microsecond-long lifetimes at cryogenic temperature, however, those in lithium halides, NaBr and NaI have relatively poor radiation efficiencies and shorter lifetimes.^{5,6} The remarkable differences of radiation efficiencies and lifetimes in two different types of host have been explained by the differences of vibronic tunneling efficiency known as the Dexter-Klick-Russell criterion.⁷⁻¹¹

As diatomic ion defects such as OH⁻ and CN⁻ have additional vibrational and rotational degrees of freedom and a large electric dipole, they may have interesting perturbation effects on the electronic properties of F* centers. In fact the emission and photoionization efficiencies of F* centers in alkali halides are reported¹²⁻¹⁶ to decrease dramatically by the presence of diatomic molecular defects such as OH⁻ and CN⁻. These interaction strengths augment with the concentration increment of molecular defects. Vibrational emission¹⁷ and anti-Stokes Raman scattering¹⁸⁻²² were observed after F center excitation in molecular defect-doped alkali halides. These previous experimental evidences have indicated that the electronic excitation energy of F centers transfers into the stretching vibrational modes of diatomic molecular defects. An F center, initially isolated from the other F and molecular defects and randomly distributed, migrates and couples with a molecular defect during optical aggregation, forming an F center-molecular defect pair, F_H center. The formation of an F_H center shifts F absorption relatively to the red wavelength in KCl, however, it splits the absorption band relatively into blue and red wavelength regions in KBr and cesium halides.^{15,23-25} This difference has been ascribed to the position and orientation differences of molecular defect to F center in F_H center.^{24,25} It has been shown¹² that F_H(OH⁻/CN⁻)* centers relax extremely rapidly and that the extremely rapid deactivation of F_H center excitation is a result of energy transfer from excited electronic F centers into the vibrational levels of the associated molecular defects *via* vibronic tunneling.

The main purpose of this work is to study the quenching processes of F* center excitation by randomly distributed OH⁻ in KCl using a picosecond technique. The quenching rates are determined by measuring ground state bleach recovery kinetic profiles of F centers as functions of OH⁻ concentration and temperature, using a picosecond streak camera absorption spectrometer. In this paper we will show experimental results to elucidate the rapid quenching processes of F center excitation by OH⁻ defects in KCl crystals. The participating roles of phonons, OH⁻ vibrations and OH⁻ dipole reorientation in the quenching processes will be also discussed.

Experimental

Materials. Single crystals of pure and OH⁻-doped KCl were additively colored and the typical mole fraction of F center is 5×10^{-5} . The actual OH⁻ concentrations in OH⁻-doped samples were determined by measuring electronic OH⁻ absorption spectra and they are at least two orders of magnitude higher than F concentration. In order to produce isolated and randomly distributed F centers, all the samples were heated to 720-770 K, cooled to room temperature immediately, mounted on the cold finger of an Air Products Liquid Transfer Heli-Tran LT-3-110 and then cooled

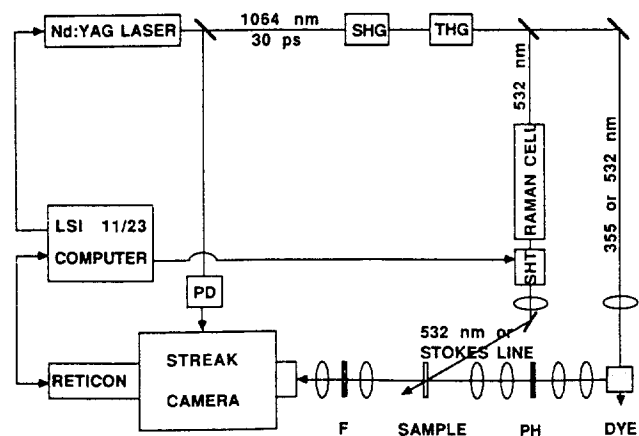


Figure 1. Schematic diagram of experimental apparatus. SHG (THG)=second (third) harmonic generator; double headed arrow=convex lens; M/C=0.25-m monochromator; F=filters; PH=pinhole; SHT=shutter; PD=photodiode.

to cryogenic temperature without light exposure. These randomly distributed samples were illuminated for optical aggregation at 240 K with the light of 550 nm from a 100-W Hg lamp with controlled exposure time. Light exposure migrates an F center toward a nearby OH⁻ defect, finally producing the associated pair of F_H(OH⁻) center. Optical aggregation brings the effect of OH⁻ concentration increment to F centers because of average interdistance reduction between F and OH⁻ defects. All the samples, if not mentioned as aggregated, are randomly distributed.

Bleach recovery profile measurements. F absorption bleach recovery profiles were obtained on the basis of a single laser shot with a picosecond transient absorption spectrometer utilizing dye emission and a streak camera,²⁶ schematically shown in Figure 1. Fluorescence from laser dye, excited by the third or second harmonic pulse with a typical energy of $\sim 10 \mu\text{J}$ of a mode-locked Quantel 471 Nd:YAG laser, was used for probe light. Samples were excited mostly by the second harmonic pulse of the laser with a typical energy of $\sim 50 \mu\text{J}$. Stokes-shifted lines of the second harmonic pulse were also generated for sample excitation using a high pressure Raman cell filled with CH₄ or SF₆ gas. The wavelength of probe light was selected by using a Jarrell Ash 0.25-m monochromator or a 10-nm band passing filter. A Hamamatsu C979 streak camera with a 10-ps time resolution, coupled to a Princeton Applied Research intensified 1420 Reticon with its 1218 multichannel controller, was used as a detector. The controller was interfaced to a Digital LSI 11/23 computer. Absorption bleach or transient absorption alters the apparent kinetic profile of dye emission seen by the streak camera. The comparison of these dye emission kinetic profiles without and with sample excitation yields an excellent picosecond absorption kinetic profile. The temporal instrument response function was determined as about 35 ps fwhm on the fastest streak rate. Rhodamine 6G was used for most bleach recovery studies and several other laser dyes were also used to check wavelength dependence. Bleach recovery times were extracted by fitting measured kinetic profiles to computer simulated recovery curves convoluted with the instrument response function. The rate is

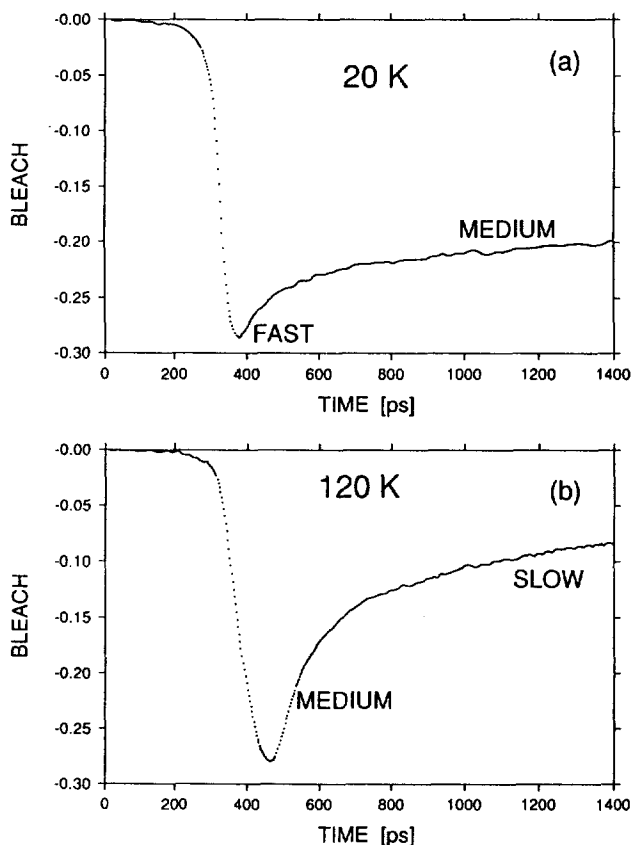


Figure 2. Typical bleach recovery profiles of F centers in OH⁻-doped KCl measured at two different temperatures (a) 20 K and (b) 120 K, revealing that three different relaxation processes can be measured with the current temporal resolution. The concentrations of F center and OH⁻ in mole fraction are $\sim 5 \times 10^{-6}$ and 2.3×10^{-3} respectively. The sample was excited at 532 nm and probed at 550+5 nm.

defined as the inverse of bleach recovery time constant.

Results and Discussion

Typical bleach recovery profiles. The bleach recovery profiles of F centers in OH⁻-doped KCl (Figure 2) show three distinguishable recovery components, designated as fast, medium and slow ones, with the current temporal resolution. Since the recovery time of each component is extremely different and the dynamic range of the streak camera absorption spectrometer at a given streak rate is limited, three recovery components can not be shown in a single recovery profile of one time window. As a result of this limited dynamic range problem, we present three recovery components in two kinetic profiles measured at two extremely different temperatures. Only the slow relaxation process is observed in OH⁻-free crystals. The bleach amplitude and rate of the medium process, which is not observed in the pure crystals, increase with OH⁻ concentration. The fast component can be observed below 40 K with the current temporal resolution in highly OH⁻-concentrated samples and in partially aggregated samples. The recovery rates of the fast and medium processes are independent of sample exci-

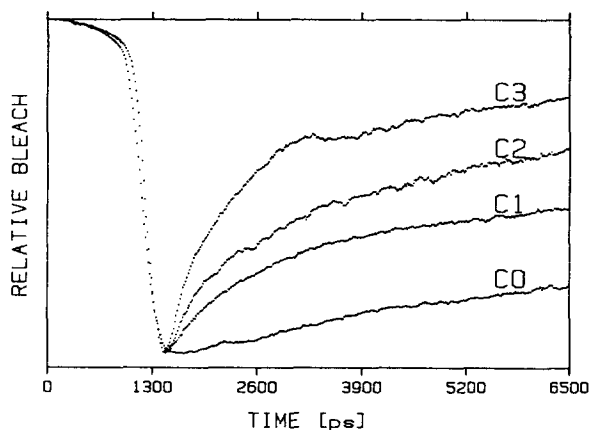


Figure 3. F absorption bleach recoveries with various OH⁻ concentrations, designating that the recovery rate of the slow component is independent of OH⁻ concentration although its relative amplitude reduces with OH⁻ concentration increment. The OH⁻ concentrations in mole fraction are 0 for C0, 6.1×10^{-4} for C1, 9.4×10^{-4} for C2 and 2.3×10^{-3} for C3, respectively.

tation laser irradiance, however, the rate of the slow one becomes faster with the increase of the irradiance.

Slow relaxation process. Figure 3 indicates that the recovery rate of the slow component is independent of OH⁻ concentration while its relative amplitude gets smaller with OH⁻ concentration increment. OH⁻-free samples have the slow relaxation process only. The relative amplitude of this process in OH⁻-doped samples reduces with temperature. The slow relaxation rates in OH⁻-doped crystals are slightly faster than the F* relaxation rate observed in the absence of OH⁻ defects. The rates are independent of OH⁻/OD⁻ isotopes. The temperature dependence of the slow relaxation rate is similar to that of F* relaxation rate found in OH⁻-free samples. Below ~ 100 K, the rate remains almost constant with temperature variation. This indicates that the main mechanism of the slow process is radiative emission at low temperature. Above 100 K, the rate increases exponentially. Activation energies using data measured above 120 K are about the same regardless of OH⁻-free samples and OH⁻/OD⁻-doped samples. The average activation energy is observed as 0.084 eV, which corresponds to the energy difference between the relaxed excited state of F center and the conduction band in KCl.^{3,27} This suggests that the mechanism of the slow relaxation process involves the thermal activation of F* electron to the conduction band followed by rapid trapping, leading to bleach recovery as found in OH⁻-free KCl.²⁷

We assert that the slow relaxation process is consequent on the normal relaxation of F* centers as known in OH⁻-free samples. The F* centers following this process relax by radiative emission at cryogenic temperature and mainly through the conduction band at high temperature. One thing to note, however, is that our measured lifetimes of the slow relaxation process below ~ 100 K seen in the time window of ~ 10 ns are shorter by a factor of 5-10 for both OH⁻-free and OH⁻-doped samples than the lifetime of F* centers previously reported for OH⁻-free KCl.²⁷ The lifetime observed in our experiments becomes smaller as sample excitation

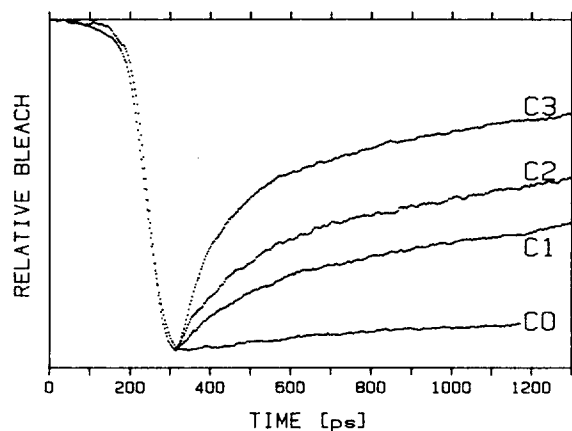


Figure 4. OH⁻ concentration-dependent recovery profiles of F absorption bleach at 120 K, showing that the relaxation rate and amplitude of the medium process grow with OH⁻ concentration increase. The respective OH⁻ concentrations for C0-C3 are the same as in Figure 3.

irradiance enlarges. The F^{*}-F^{*} self annihilation interaction could produce an additional quenching mechanism since the large population of F^{*} centers is instantly generated by high peak power laser pulses in our picosecond experiment. The slight increase of the rate in highly OH⁻-doped samples may result from the gross effect of doping which might perturb, for example, the thermal activation energy to the conduction band. Or, in the self annihilation interaction of F^{*} center, the excess energy of the electron jumped to the conduction band could be removed by OH⁻-vibrational absorption.

Medium relaxation process. The concentration dependence of the medium process in Figure 4 shows that the rate and amplitude of the medium process enlarge with OH⁻ concentration. OH⁻-free samples do not show this process. It is apparent from OH⁻ concentration dependence that medium process is resulted from direct coupling between F^{*} center and OH⁻ defect. The amplitude as well as rate of the medium process increases with temperature. The temperature-dependent quenching efficiency of steady-state emission and photoionization¹⁵ is now turned out to be determined mostly by the rate and amplitude variations of the medium process. Figure 5 reveals the temperature dependence of the medium relaxation rate at three different OH⁻ concentrations. Below ~90 K, the rate increases linearly with temperature. So the medium relaxation process is assisted predominantly by one phonon processes below 90 K.²⁸ Above ~90 K, the rate grows exponentially with temperature. The relaxation rates measured above ~90 K show a good linearity within our experimental error in Arrhenius plots for both OH⁻- and OD⁻-doped samples. Average activation energies of 400 and 300 cm⁻¹ were obtained for OH⁻- and OD⁻-doped samples respectively. These observed activation energies correspond to the librational energies of OH⁻ and OD⁻ respectively in KCl.²⁹⁻³¹ The basic librational energy of OH⁻ in KCl is reported as ~300 cm⁻¹ and that of OD⁻ is reduced by a factor of ~1.3.^{29,30} The librational bands have broad Lorentzian shapes even at liquid helium temperature and they broaden more rapidly on the high energy side as temperature increases.²⁹ The librational energies with

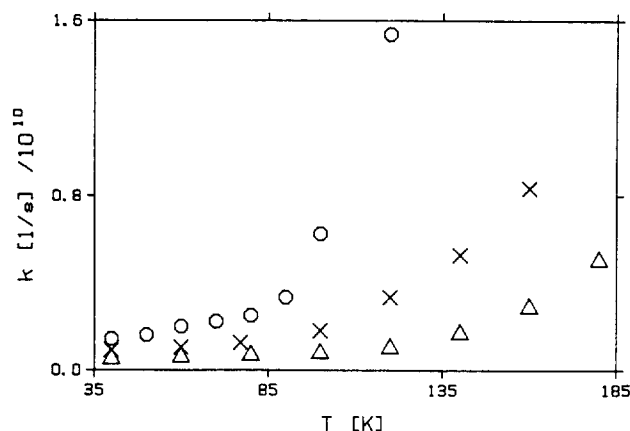


Figure 5. Temperature dependences of the medium recovery rate. The molecular defect concentrations in mole fraction are 2.3×10^{-3} OH⁻ for (○), 1.8×10^{-3} OD⁻ for (×) and 9.4×10^{-4} for (△), respectively.

weaker excitation are reported³² to exist also at higher energies of 383 and 407 cm⁻¹ for OH⁻ in KCl.

The quenching efficiency is reported³³ to be higher in KCl than in RbCl or KBr for the same OH⁻ concentration and to increase with T⁴, suggesting that the quenching might be assisted by OH⁻ dipole reorientation. OH⁻ dipole reorientation rate in KCl is ~100 times higher than those in RbCl and KBr.³³ It is reported^{32,34-36} in alkali halides that below 5 K the reorientation rate of OH⁻ dipole grows linearly with temperature, assisted predominantly by one phonon processes, while above 5 K the rate increases proportionally to T⁴, assisted predominantly by multi-phonon processes. However, a direct correlation of quenching efficiency to quenching rate is wrong since the amplitude as well as rate of the medium process changes with temperature and the medium process is not the only quenching process of F excitation. Nevertheless, the medium process seems to be favored along with OH⁻ dipole reorientation in some way.

The medium process is assisted mainly by one phonon processes below 90 K, however, above 90 K, mainly by more efficient OH⁻-librational motions. Assurances by OH⁻ librations, OH⁻ dipole reorientations and/or lattice vibrations are required for the medium process to mix the excited state character of OH⁻ as well as to compensate for the energy mismatch between donor and acceptor. The mixing of the OH⁻-excited states into the ground state with the assistances of OH⁻ libration, dipole reorientation and lattice vibrations might be essential for the medium process since the distance between F^{*} and OH⁻ is relatively large. The perturbed ground state of OH⁻ with some characters of excited states, which have Rydberg orbital characters, might cross with the excited state orbital of F center, resulting in energy transfer from F^{*} centers to OH⁻-vibrational levels. The E-V energy transfer to OH⁻ following this medium recovery component might be correlated to the reported²¹ anti-Stokes Raman line of 3650 cm⁻¹. This Raman line was suggested²¹ to result from energy transfer between a widely separated F^{*}·OH⁻ pair, characterized by the frequency nearly equal to that of isolated OH⁻ ion²² and by a slightly weaker E-V transfer process so that only the $\nu=1$ state is populated.

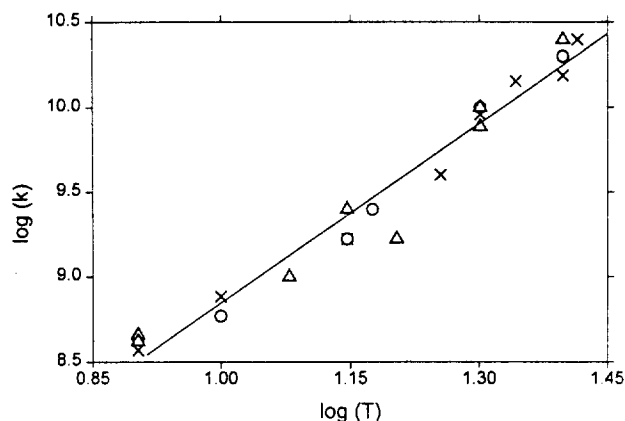


Figure 6. Temperature dependence of the fast relaxation rate. The molecular defect concentrations in mole fraction are 2.3×10^{-3} OH^- for (x), 1.8×10^{-3} OD^- for (o) and 2.3×10^{-3} OD^- for (Δ), respectively. The slope determined in this double logarithmic plot, using all the datum points, is 3.5.

Fast relaxation process. The fast process is negligible compared with the other relaxation processes in randomly distributed samples with a lower OH^- concentration than 10^{-3} in mole fraction. The fast relaxation amplitude increases with the OH^- concentration but this process is a minor relaxation process yet for any samples we studied. The rate of this process is observed to be independent of OH^- concentration within experimental errors. Figure 6 shows the temperature dependence of the fast relaxation rates in randomly disordered samples with different OH^-/OD^- concentrations. High experimental errors are inherently involved in the measurement of this rate because of its small amplitude. However, the relaxation rates seem to be about the same regardless of OH^-/OD^- concentration and aggregation. No isotope effect was observed for the rate or amplitude of this process. The slope was determined as 3.5 from the double logarithmic plot of Figure 6. The temperature dependence of the fast relaxation rate, as T^3 - T^4 , suggests that this process is assisted by multi-phonon processes.³⁵ The electron cloud of F^* center following this fast relaxation process is suggested to overlap with the orbitals of OH^- defects. The surface crossing without introducing excited state characters by OH^- librations or dipole reorientations enables energy transfer to be fast even at low temperature, with the assistance of multi-phonon processes to remove excess energy during energy transfer.

The E-V energy transfer to OH^- following by this fast recovery component could be related to the reported²² anti-Stokes Raman lines of 3600 and 3410 cm^{-1} , which were attributed to the $\nu=1 \rightarrow 0$ and $\nu=2 \rightarrow 1$ OH^- -vibrational transitions in $\text{F}_\text{H}(\text{OH}^-)$ complex. The presence of a soft F center neighbor lowers slightly the OH^- -stretching frequency relatively to that of isolated defect.²³ The independences of the OH^-/OD^- concentration and aggregation for the fast recovery rate suggest that the distances between F^* and OH^- are the same for the F^* centers following the fast relaxation process. However, this is not sufficient to indicate that the fast recovery component is owing to the relaxation of $\text{F}_\text{H}(\text{OH}^-)^*$ centers since we observe that the bleach amplitudes

of OH^- -doped samples decrease with optical aggregation, however, those of pure samples do not. This bleach amplitude decrease indicates that $\text{F}_\text{H}(\text{OH}^-)$ centers formed by optical aggregation relax too fast to be observed with the current temporal resolution. In fact $\text{F}_\text{H}(\text{OH}^-)^*$ centers are reported¹² to relax in ~ 3 ps in KCl. Nonetheless, there is same possibility that this fast process is due to the relaxation of some type of $\text{F}_\text{H}(\text{OH}^-)^*$ centers. Two different configurations of $\text{F}_\text{H}(\text{OH}^-)$ centers are known in KBr and KI.³⁷ The further wavelength shift to the red by optical aggregation suggests a hypothesis that the optical aggregation forms the $\text{F}_\text{H}(\text{OH}^-)_\text{II}$ centers where F centers are on the parallel orientation with OH^- ellipsoidal elastic dipole tensor³⁷ since parallel orientation induces redder shift because of better hydrogen bonding. Then the fast component might be due to the relaxation of $\text{F}_\text{H}(\text{OH}^-)_\text{I}$ centers where F centers are on the vertical orientation to OH^- dipole tensor. However, to confirm this hypothesis and to understand the E-V energy transfer process better, it is necessary to study more thoroughly with a better temporal resolution. For the present we rather suggest that relaxation of somewhat distant, not the most closest, associated pairs of F^* and OH^- yields the fast component.

Overall relaxation processes and summary. The bleach recovery kinetic studies of randomly distributed F centers in KCl with variations of OH^- concentration, isotope and temperature have revealed many new observations which may provide new insights to understand electronic interactions between F^* centers and diatomic molecular defects. The main observations can be summarized as follows.

(1) The F center bleach in OH^- -doped crystals shows three distinguishable recovery components, designated as slow, medium and fast ones, with the current experimental resolution. The slow process is ascribed to the normal relaxation of F^* centers as known in OH^- -free samples. The other processes result from energy transfer from F^* centers to OH^- -vibrational energy levels.

(2) The F^* centers showing the slow component relax by radiative emission at low temperature and mainly through the conduction band at high temperature.

(3) The fast component comes from the relaxation of the F^* center that is associated to OH^- with some distance.

(4) OH^- librations, OH^- dipole reorientations and certain lattice vibrations assist the energy transfer of the medium component between widely separated F^* and OH^- defects. The quenching behaviors of steady state F^* luminescence and photoionization by OH^- are explained well by the medium relaxation process.

Acknowledgment. We are very grateful to Professor M. A. El-Sayed, School of Chemistry and Biochemistry, Georgia Institute of Technology for allowing this experiment to be carried out in his lab with very helpful discussion and for allowing this work to be published without his name. We also thank for Professor F. Luty, Physics Department, University of Utah for providing samples. This work was financially supported by the S.N.U. Daewoo Research Fund and the Korean Ministry of Education.

References

1. Chung, Y. B.; Lee, I. W.; Jang, D.-J. *Opt. Commun.* **1991**,

- 86, 41.
2. Baldacchini, G.; Pan, D. S.; Luty, F. *Phys. Rev. B* **1981**, *24*, 2174.
3. Markham, J. J. In *F Centers in Alkali Halides*; Academic Press: New York, U.S.A., 1966; p 1.
4. De Matteis, F.; Leblans, M.; Joosen, W.; Schoemaker, D. *Phys. Rev. B* **1992**, *45*, 10377.
5. Honda, S.; Tomura, M. *J. Phys. Soc. Jpn.* **1972**, *33*, 1003.
6. Bosi, L.; Bussolati, C.; Spinolo, G. *Phys. Rev. B* **1970**, *1*, 890.
7. Dexter, D. L.; Klick, C. C.; Russell, G. A. *Phys. Rev.* **1955**, *100*, 603.
8. Gomes, L.; Morato, S. P. *J. Appl. Phys.* **1989**, *66*, 2754.
9. Bartram, R. H.; Stoneham, A. M. *Solid State Commun.* **1975**, *17*, 1593.
10. De Matteis, F.; Leblans, M.; Schoemaker, D. *Phys. Rev. B* **1994**, *49*, 9357.
11. De Matteis, F.; Leblans, M.; Sloomans, W.; Schoemaker, D. *Phys. Rev. B* **1994**, *50*, 13186.
12. Jang, D.-J.; Lee, J. *Solid State Commun.* **1995**, *94*, 539.
13. Casalboni, M.; Proposito, P.; Grassano, U. M. *Solid State Commun.* **1993**, *87*, 305.
14. Jang, D.-J.; Corcoran, T. C.; El-Sayed, M. A.; Gomes, L.; Luty, F. In *Ultrafast Phenomena V*; Fleming, G. R.; Siegman, A. E., Ed.; Springer-Verlag: Berlin, 1986; p 280.
15. Gomes, L.; Luty, F. *Phys. Rev. B* **1984**, *30*, 7194.
16. Yang, Y.; Luty, F. *Phys. Lett.* **1983**, *51*, 419.
17. Yang, Y.; von der Osten, W.; Luty, F. *Phys. Rev. B* **1985**, *32*, 2724.
18. Halama, G.; Lin, S. H.; Tsen, K. T.; Luty, F.; Page, J. B. *Phys. Rev. B* **1990**, *41*, 3136.
19. Tsen, K. T.; Halama, G.; Luty, F. *Phys. Rev. B* **1987**, *36*, 9247.
20. Halama, G.; Tsen, K. T.; Lin, S. H.; Page, J. B. *Phys. Rev. B* **1991**, *44*, 2040.
21. Cachei, G.; Stoltz, H.; van der Osten, W.; Luty, F. *J. Phys. Condens. Matter* **1989**, *1*, 3239.
22. Halama, G.; Tsen, K. T.; Lin, S. H.; Luty, F.; Page, J. B. *Phys. Rev. B* **1989**, *39*, 13457.
23. Krantz, M.; Luty, F. *Phys. Rev. B* **1988**, *37*, 8412.
24. Krantz, M.; Luty, F.; Dierolf, V.; Paus, H. *Phys. Rev. B* **1991**, *43*, 9888.
25. Sothe, H.; Spaeth, J.-M.; Luty, F. *J. Phys. Condens. Matter* **1993**, *5*, 1957.
26. Jang, D.-J.; Kelley, D. F. *Rev. Sci. Instrum.* **1985**, *56*, 2205.
27. Luty, F. In *Physics of Color Centers*; Fowler, W. B., Ed.; Academic Press: New York, U.S.A., 1968; p 182.
28. Holstein, T.; Lyo, S. K.; Orbach, R. *Phys. Rev. B* **1977**, *6*, 934.
29. Klein, M. V.; Wedding, B.; Levine, M. A. *Phys. Rev. B* **1969**, *180*, 902.
30. Wedding, B.; Klein, M. V., *Phys. Rev.* **1969**, *177*, 1274.
31. Harrison, D. *Ph. D. Thesis*; Univ. of Utah: Salt Lake City, U.S.A., 1970; p 1.
32. Kapphan, S.; Luty, F. *Solid State Commun.* **1970**, *8*, 349.
33. Gomes, L.; Luty, F. In *Proceedings of the International Conference on Defects in Insulating Crystals*; Salt Lake City, U.S.A., 1984; p 182.
34. Narayananmurti, V.; Pohl, R. O. *Rev. Mod. Phys.* **1970**, *42*, 201.
35. Kapphan, S. *J. Phys. Chem. Solids* **1974**, *35*, 621.
36. Bridges, F. *CRC Crit. Rev. Solid State Sci.* **1975**, *5*, 1.
37. Baldacchini, G.; Botti, S.; Grassano, U. M.; Gomes, L.; Luty, F. *Europhys. Lett.* **1989**, *9*, 735.

Prediction of Lipophilicity of Orthopramides by Comparative Molecular Field Analysis (CoMFA)

Sung-eun Yoo* and Young Ah Shin

Korea Research Institute of Chemical Technology, Daedeog Science Complex, Taejeon 305-606, Korea

Received August 18, 1995

The comparative molecular field analysis (CoMFA) method has been employed to correlate the apparent lipophilicity ($\log k_w$) and global lipophilicity ($\log P$) for orthopramide derivatives. This study demonstrated that CoMFA is an excellent method in predicting the complex properties of molecules such as apparent lipophilicity ($\log k_w$) or lipophilicity ($\log P$). The better predictability of lipophilicity by introducing $\log k_w$ as an independent descriptor suggests that the HPLC capacity factor measured in a buffer of pH 7.5 ($\log k_w$) can be effectively utilized in the prediction of global lipophilicity.

Introduction

Comparative Molecular Field Analysis (CoMFA),¹ a new 3-D QSAR (quantitative structure-activity relationship) approach developed by Cramer *et al.*, has become a popular and valuable tool in drug design.² Traditional QSAR attempts to correlate the biological properties of a series of molecules

with the physicochemical property which are normally derived empirically. However, the CoMFA method tries to correlate the target variables with more fundamental properties of the molecules, steric and electrostatic properties. These properties are calculated theoretically and thus, CoMFA does not require predetermined physicochemical parameters for the analysis. Moreover, classical 2D-QSAR is applied only